The *Caenorhabditis elegans* GARP complex contains the conserved Vps51 subunit and is required to maintain lysosomal morphology

L. Luo[a], M. Hannemann[a], S. Koenig[a,b], J. Hegermann[a,b], M. Ailion[c], M.-K. Cho[d], N. Sasidharan[a], M. Zweckstetter[b,d], S. A. Rensing[e], and S. Eimer[a,b]

[a]European Neuroscience Institute, 37077 Göttingen, Germany; [b]DFG Research Center for Molecular Physiology of the Brain, University Medical Faculty, 37073 Göttingen, Germany; [c]Department of Biology, University of Utah, Salt Lake City, UT 84112; [d]NMR Based Structural Biology, Max-Planck Institute for Biophysical Chemistry, 37077 Göttingen, Germany; [e]Faculty of Biology, University of Freiburg, 79085 Freiburg, Germany

ABSTRACT **In yeast the Golgi-associated retrograde protein (GARP) complex is required for tethering of endosome-derived transport vesicles to the late Golgi. It consists of four subunits—Vps51p, Vps52p, Vps53p, and Vps54p—and shares similarities with other multimeric tethering complexes, such as the conserved oligomeric Golgi (COG) and the exocyst complex. Here we report the functional characterization of the GARP complex in the nematode *Caenorhabditis elegans*. Furthermore, we identified the *C. elegans* Vps51 subunit, which is conserved in all eukaryotes. GARP mutants are viable but show lysosomal defects. We show that GARP subunits bind specific sets of Golgi SNAREs within the yeast two-hybrid system. This suggests that the *C. elegans* GARP complex also facilitates tethering as well as SNARE complex assembly at the Golgi. The GARP and COG tethering complexes may have overlapping functions for retrograde endosome-to-Golgi retrieval, since loss of both complexes leads to a synthetic lethal phenotype.**

Monitoring Editor
Adam D. Linstedt
Carnegie Mellon University

Received: Jun 8, 2010
Revised: May 2, 2011
Accepted: May 13, 2011

INTRODUCTION

Vesicular membrane transport between different intracellular compartments relies on the specific delivery and fusion of transport containers with the acceptor membrane. Although *N*-ethylmaleimide–sensitive factor attachment receptor (SNARE) proteins are sufficient to execute membrane fusion in purified membrane fusion assays in vitro, cells require additional factors for efficient vesicular membrane trafficking in vivo (Lang and Jahn, 2008). In particular, it is still not clear how specificity is achieved during membrane transport. A set of additional factors helps to make the match by tethering transport vesicles to the acceptor membrane. These factors also confer specificity for the fusion process by bringing the SNARE proteins in close proximity to allow efficient SNARE pairing. Tethering factors can be divided into two groups: 1) long coiled-coil proteins and 2) multisubunit tethering complexes. Long coiled-coil proteins are recruited to acceptor membranes mostly by small GTPases and mark the identity of domains on subcellular compartments (Short *et al.*, 2005). Multimeric tethering complexes are also bound by small GTPases in their active, GTP-bound form and cooperate with the long coiled-coil proteins to tether vesicles to the acceptor membrane (Whyte and Munro, 2002). Three of these multisubunit tethering complexes share similarities in their domain architecture and are composed of multimers of fourfold-symmetric components. Therefore they were termed "quatrefoil" tethering complexes. This group consists of the exocyst, the conserved oligomeric Golgi (COG) complex, and the Golgi-associated retrograde protein (GARP) complex (Whyte and Munro, 2002). The exocyst contains eight subunits, is required for tethering of vesicles to the plasma membrane, and localizes mainly to sites of polarized growth (Hsu *et al.*, 2004). In contrast, COG and GARP complexes are thought to function mainly in retrograde transport. The COG complex has been shown to tether vesicles to the Golgi apparatus (Bruinsma *et al.*, 2004; Ungar *et al.*, 2006; Shestakova *et al.*, 2007; Smith *et al.*, 2009). It contains eight subunits that are organized in two subcomplexes. COG1–4 are required for viability in yeast, whereas

This article was published online ahead of print in MBoC in Press (http://www.molbiolcell.org/cgi/doi/10.1091/mbc.E10-06-0493) on May 25, 2011.

Address correspondence to: Stefan Eimer (seimer@gwdg.de).

Abbreviations used: COG, conserved oligomeric Golgi complex; GARP, Golgi associated retrograde protein complex; SNARE, soluble N-ethylmaleimide-sensitive factor attachment receptor; TGN, *trans*-Golgi network; VPS, vacuolar protein sorting protein.

COG5–8 are not (Whyte and Munro, 2002; Ungar *et al.*, 2006). The COG complex has been proposed to act at multiple retrograde transport steps within the Golgi as well as from post-Golgi, endosomal compartments to the Golgi (Bruinsma *et al.*, 2004; Shestakova *et al.*, 2007; Smith *et al.*, 2009). A retrieval function within the Golgi–endosomal interface was also suggested by the fact that COG activity is required for proper localization of proteins to the *trans*-Golgi network (TGN) (Spelbrink and Nothwehr, 1999) and early Golgi (Bruinsma *et al.*, 2004).

In contrast to the COG complex, the GARP complex seems not to be involved in intra-Golgi retrograde transport but has been reported to tether endosome-derived vesicles to the Golgi. In yeast, the GARP complex consists of four subunits: Vps51p, 52p, 53p, and 54p. It localizes to the TGN and has been shown to be required for protein sorting at the Golgi–endosomal interface (Conboy and Cyert, 2000; Conibear and Stevens, 2000; Conibear *et al.*, 2003; Siniossoglou and Pelham, 2002; Reggiori *et al.*, 2003). Specifically, the retrieval of late Golgi membrane proteins, TGN cargo receptors, and SNAREs is defective in GARP mutants. The GARP complex is an effector of the Rab GTPase Ypt6p and the Arf-like GTPase Arl1 (Siniossoglou and Pelham, 2001, 2002; Conibear *et al.*, 2003; Panic *et al.*, 2003; Liewen *et al.*, 2005). It also interacts with the late Golgi SNARE Tlg1p (Siniossoglou and Pelham, 2001, 2002; Conibear *et al.*, 2003; Reggiori *et al.*, 2003; Liewen *et al.*, 2005).

Like the other tethering complexes, the GARP complex is evolutionarily conserved. However, only Vps52, 53, and 54 had been identified in metazoans and shown to assemble a stable complex (Liewen *et al.*, 2005; Perez-Victoria *et al.*, 2008). Knockdown of GARP components by RNAi leads to missorting of the lysosomal hydrolase cathepsin D by lack of retrieval of its cargo receptor to the late Golgi. Similar to yeast, it has also been shown that TGN proteins like TGN46 were mislocalized due to a lack of recycling back to the Golgi (Perez-Victoria *et al.*, 2008). Furthermore, specific mutations in Vps54 cause motoneuron degeneration and sperm defects in mice (Schmitt-John *et al.*, 2005).

To study the requirement of GARP-mediated Golgi retrieval for a multicellular organism, we used *Caenorhabditis elegans* to analyze GARP complex function.

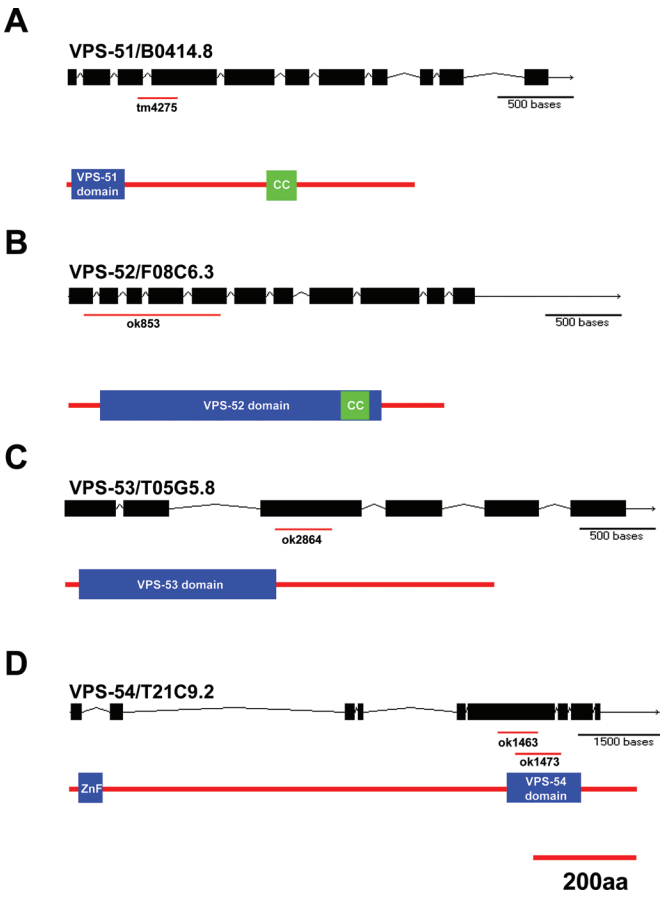

FIGURE 1: The subunits of the *C. elegans* GARP complex. The gene structure and protein structures of the four *C. elegans* GARP subunits VPS-51 (A), VPS-52 (B), VPS-53 (C), and VPS-54 (D) are shown. The exon–intron structure of each gene is depicted by solid black bars (exons), which are connected by thin lines (introns). The positions of the respective deletion alleles are given by red lines below the gene structures. The domain organization of the different GARP subunits is shown below the gene structures. CC, coiled-coil; ZnF, zinc finger.

RESULTS

Identification of the GARP complex in *C. elegans* and cloning of the VPS-51 subunit

GARP complex function has been described in yeast and mammalian cell culture. To study the function of the GARP complex in a multicellular organism, we identified orthologues of the different subunits in the nematode *C. elegans* (Figure 1). Previously it was been suggested that the mammalian GARP complex contains just the three subunits Vps52, Vps53, and Vps54 (Liewen *et al.*, 2005; Koumandou *et al.*, 2007; Perez-Victoria *et al.*, 2008), unlike yeast, in which Vps51p had also been identified. By using the minimal conserved protein domain described for the yeast Vps51p we generated an alignment of all the yeast Vps51 family members. Using the Vps51 domains from *Dictyostelium discoideum* (amino acids 182–262) and *Neurospora crassa* (amino acids 250–310) (Figure 2E), we searched the *C. elegans* protein databases by iterated Basic Local Alignment Search Tool searches. These searches revealed a specific match to the uncharacterized *C. elegans* open reading frame (ORF) B0414.8 with 30% identity/65% similarity to *Dictyostelium* and 36% identity/68% similarity to *Neurospora*, respectively. Comparisons with *Drosophila*, *Arabidopsis*, and the mammalian system revealed that this Vps51 domain has a characteristic central LVYENYNK-FISATDT motif that distinguishes it from the common motifs found with COG or exocyst subunits. Extensive multiple sequence alignments extended this central Vps51 consensus motif as shown in Supplemental Figure 1D. This domain had been independently identified as a Dor1-like domain and shown to be closely related to the COG and exocyst subunits Cog8 and Sec5 (Whyte and Munro, 2001). However, this newly identified class of proteins was not linked to the GARP complex. Because the COG and exocyst subunits have been identified in *C. elegans*, we reasoned that ORF B0414.8 might encode the missing VPS-51 subunit of the GARP complex (Figure 1). To see whether B0414.8 colocalizes with the rest of the GARP complex, we expressed a translational mCherry-B0414.8 fusion protein and determined its localization relative to the other GARP subunits. As shown in Figure 2A, the localization of mCherry-B0414.8 completely overlapped with that of VPS-52-mYFP, as well as with the other subunits (unpublished data). All fluorescently tagged GARP subunits showed perfect colocalization with each other (Figure 2A). To further demonstrate that B0414.8 is indeed an integral part of the *C. elegans* GARP complex, we coimmunoprecipitated the other subunits with B0414.8 and vice versa (Figure 2B). These interactions were specific, since it was not possible to coimmunoprecipitate an mCherry-Rab-2 fusion protein with any of the GARP subunits

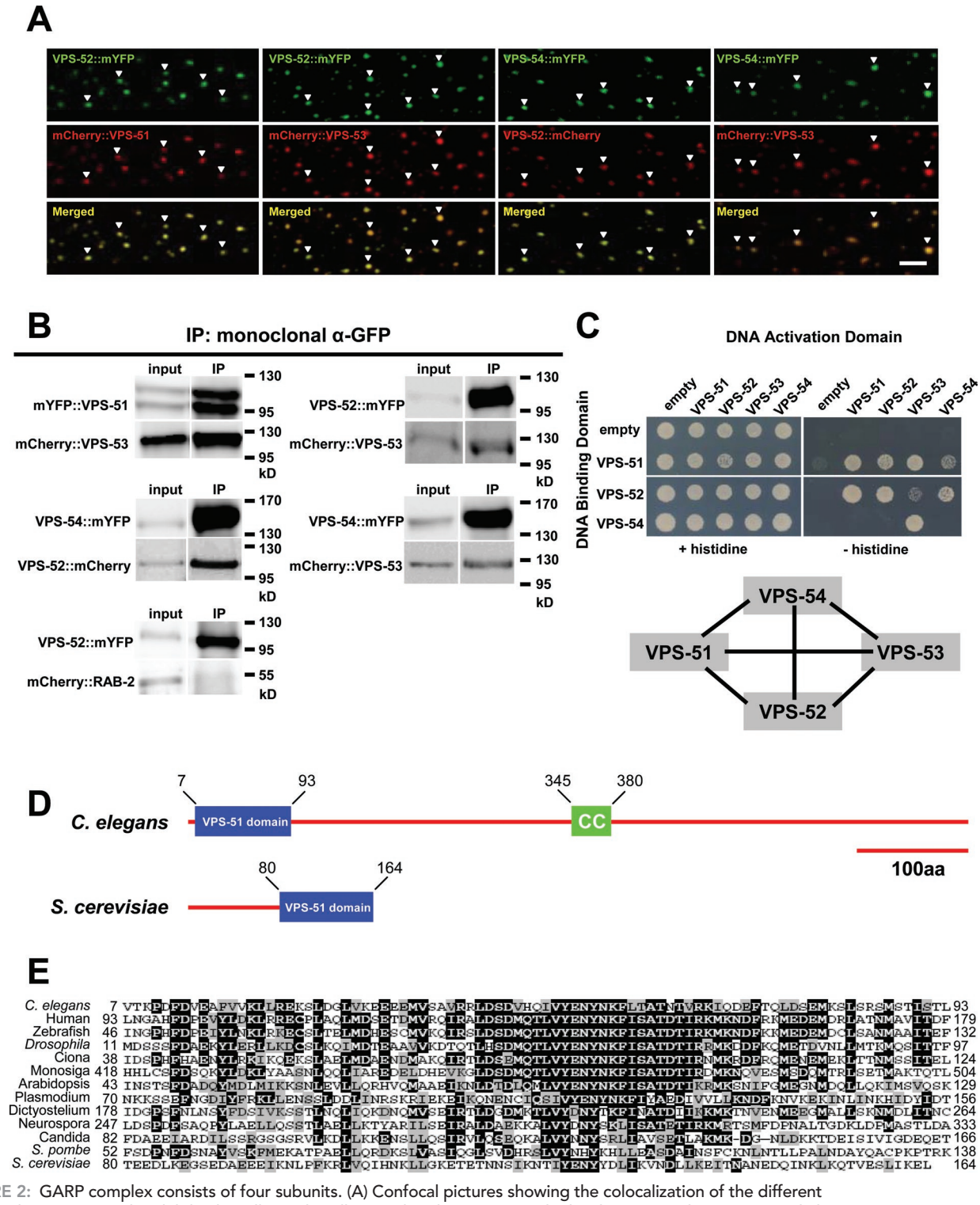

FIGURE 2: GARP complex consists of four subunits. (A) Confocal pictures showing the colocalization of the different GARP subunits in a single adult body-wall muscle cell. Arrowheads point to similar localizations in the images. Scale bar, 5 μm. (B) Coimmunoprecipitations were performed from mixed-stage extracts of transgenic animals expressing combinations of mYFP- and mCherry-tagged GARP subunits as indicated. One percent of each extract used for immunoprecipitation was loaded as input. The monoclonal anti-GFP antibodies used for immunoprecipitations recognized mYFP but not mCherry. The concentrated mYFP-fused proteins were detected by polyclonal anti-GFP antibodies, which recognize mYFP but not mCherry. The coimmunoprecipitated products were detected with polyclonal anti-DsRed antibodies, which recognize mCherry but not mYFP. A GARP subunit tagged with mCherry can be copurified with another GARP subunit tagged with mYFP, indicating physical interactions between GARP subunits. A combination of VPS-52-mYFP and mCherry-RAB-2 was used as a negative control. (C) Interaction between GARP subunits as determined by yeast two-hybrid assays. The growth medium without histidine selects for interactions. (D) Schematics of VPS-51 domains in *C. elegans* and *S. cerevisiae*; CC, coiled coil domain. (E) Alignment of VPS-51 domains from different species. Conserved amino acids are boxed in black and similar ones in gray.

expressed in the same body-wall muscle cells as a control (unpublished data; Figure 2B). In addition, all GARP subunits also display interactions with each other and B0414.8/VPS-51 when assayed in the yeast two-hybrid system (Figure 2C). This strongly suggests that the metazoan GARP complex has four subunits, as in yeast, and that B0414.8 is the missing VPS-51 subunit.

Vps51 is evolutionarily conserved and present in all eukaryotic organisms

In contrast to the 164–amino acid (aa) yeast *Saccharomyces cerevisiae* Vps51p, *C. elegans* VPS-51 consists of 700 aa. Except for the Vps51 homology domain (Figure 2D) and a coiled-coil motif, there are no clearly recognizable domains present in VPS-51 (Figure 1A). By using the newly identified Vps51 domain (see Supplemental Figure S1), we were able to identify clear Vps51 orthologues in all eukaryotic organisms. The Vps51 orthologue group is phylogenetically separated from the COG and exocyst subunits (Supplemental Figure S1, A–D). In contrast to the yeast family, Vps51 proteins are around 700–900 aa in plants and animals and 700–1700 aa in the different protist lineages of heterologous single-celled eukaryotes ranging from *Monosiga* and *Dictyostelium* to *Plasmodium* and *Trypanosoma*. Human Vps51 has been previously identified as "another new gene 2" (ANG2) protein or C11orf2 (O'Brien *et al.*, 2000) and has recently been shown to be part of the mammalian GARP complex (Perez-Victoria *et al.*, 2010). The Vps51 protein from zebrafish, named *fat-free* (*ffr*), has been identified and shown to be required for intestinal lipid absorption and proper Golgi morphology (Ho *et al.*, 2006). Almost all Vps51 proteins have the same domain architecture, with the Vps51 domain at the N-terminus and no recognizable domains except some coiled-coil regions C-terminally (Figure 1E and Supplemental Figure S1E). Among metazoan Vps51 proteins, motif detection revealed several conserved regions beside the Vps51 domain that are present in almost all Vps51 proteins (Supplemental Figure S1, D and E). This suggests that a common ancestor possessed a GARP complex containing a large Vps51 subunit and that all subsequent alterations—for example, the truncation of Vps51 in the yeast family—were caused by secondary sequence loss during evolution. The truncations and low similarity between the yeast and metazoan Vps51 proteins (Figure 2E) might explain why it was difficult to identify Vps51 in the metazoan system.

The *C. elegans* GARP complex localizes to Golgi domains

Transcriptional fusions of the *vps-51*, *-52*, and *-53* promoters to green fluorescent protein (GFP) revealed that the GARP complex subunits are ubiquitously expressed, with particularly strong expression in neuronal cells (Supplemental Figure S2). This suggests that GARP complex activity is required in many cell types, as in mammals (Liewen *et al.*, 2005). Localization studies using fluorescently tagged GARP subunits showed that the *C. elegans* GARP complex extensively colocalizes in body-wall muscle cells with medial Golgi markers such as α-mannosidase II and a GFP-tagged GRIP domain from the *trans*-Golgi golgin T05G5.9 (Figure 3A). VPS-52-mCherry showed a more partial overlap with endosomal domains labeled by the phosphoinositol-3-phosphate–binding GFP-2xFYVE domain fusion (Figure 3A). This is consistent with the findings in yeast and mammals that the GARP complex localizes to the late Golgi (Conboy and Cyert, 2000; Conibear and Stevens, 2000; Perez-Victoria *et al.*, 2008) and endosomal compartments, as well as vesicular structures distributed throughout the cell body (Liewen *et al.*, 2005). In *C. elegans* body-wall muscles, only Golgi ministacks are present (~200 nm diameter). Because they form an integral unit with an endoplasmic reticulum (ER) exit site and endosomal compartment (Figure 3B), colocalization might reflect the diffraction-limited localization of two fluorescence signals to the same secretion unit. Therefore we reanalyzed the localization of the GARP complex in macrophage-like coelomocytes in *C. elegans*, which contain mostly a series of parallel Golgi stacks of ~500–800 nm in size (Figure 3D). In coelomocytes, the fluorescently tagged GARP subunit VPS-52-tagRFP showed perfect overlap with the medial Golgi marker Mans-GFP, but there was no colocalization detectable between VPS-52-tagRFP and the endosomal marker 2xFYVE-GFP (Figure 3C). This suggests that the GARP complex localizes to the Golgi complex.

The yeast GARP complex is recruited to Golgi membranes by the Rab6 GTPase Ypt6p. In *C. elegans* the staining of fluorescently tagged GARP complex subunits also largely overlapped with the staining seen for the two *C. elegans* Rab6 orthologues, RAB-6.1 and RAB-6.2 (Figure 3E). Consistent with previous reports, we were able to coimmunoprecipitate the GARP complex with both Rab6 GTPases in *C. elegans* (Figure 3F). This interaction was specific, since we were not able to coimmunoprecipitate any of the GARP subunits with a GFP-tagged RAB-10 as a control (Figure 3F). This demonstrates that the *C. elegans* GARP complex also binds Rab6, as in yeast and mammals (Siniossoglou and Pelham, 2001; Liewen *et al.*, 2005). Whether *C. elegans* Rab6 is also required to recruit the GARP complex to the Golgi could not be tested because inactivation of both RAB-6 molecules leads to lethality.

In yeast it has also been demonstrated that if one of the core subunits Vps52p, 53p, or 54p is missing, the remaining subunits are rendered unstable and are degraded (Conibear and Stevens, 2000). To test whether the *C. elegans* complex behaves similarly, we determined the stability and localization of the remaining core GARP subunits when one is deleted. As shown in Figure 1, there are deletion mutants available for all GARP subunits in *C. elegans*. All deletions lead to frame shifts and early stop codons that truncate the proteins before the coiled-coil regions that are required for complex incorporation (Siniossoglou and Pelham, 2002; Perez-Victoria *et al.*, 2008). Therefore these deletions should correspond to strong loss of function and most likely resemble molecular null alleles. In agreement with this, we were never able to enhance any of the observed phenotypes in double- or triple-mutant combinations of the GARP subunits (unpublished data; Figure 5A later in the paper). To our surprise, deletion of any of the four GARP complex subunits in *C. elegans* did not lead to a mislocalization of the remaining subunits (Figure 4A) or to their instability as assayed by Western blot analysis (Figure 4B). So far it has only been reported that the yeast Vps51p subunit is dispensable for core complex localization and stability (Siniossoglou and Pelham, 2002; Conibear *et al.*, 2003).

To understand the reason for this difference, we analyzed possible interactions between the different GARP subunits in *C. elegans* by yeast two-hybrid assays. On the basis of our finding, it might be expected that each subunit would display multiple interactions within the complex, as has been suggested for the mammalian GARP complex (Liewen *et al.*, 2005; Perez-Victoria *et al.*, 2008). In agreement with this, all *C. elegans* GARP subunits display interactions with each other when assayed in the yeast two-hybrid system (Figure 2C). This creates a complex VPS-51-52-53-54 interaction network within the *C. elegans* GARP complex, suggesting that even in the absence of a subunit the remaining subunits may still interact and localize properly. In addition, it is also possible that isolated subunits or subcomplexes have independent means to localize to the Golgi–endosomal interface. Therefore it was important to test the functional activity of the remaining GARP subunits when one subunit is missing.

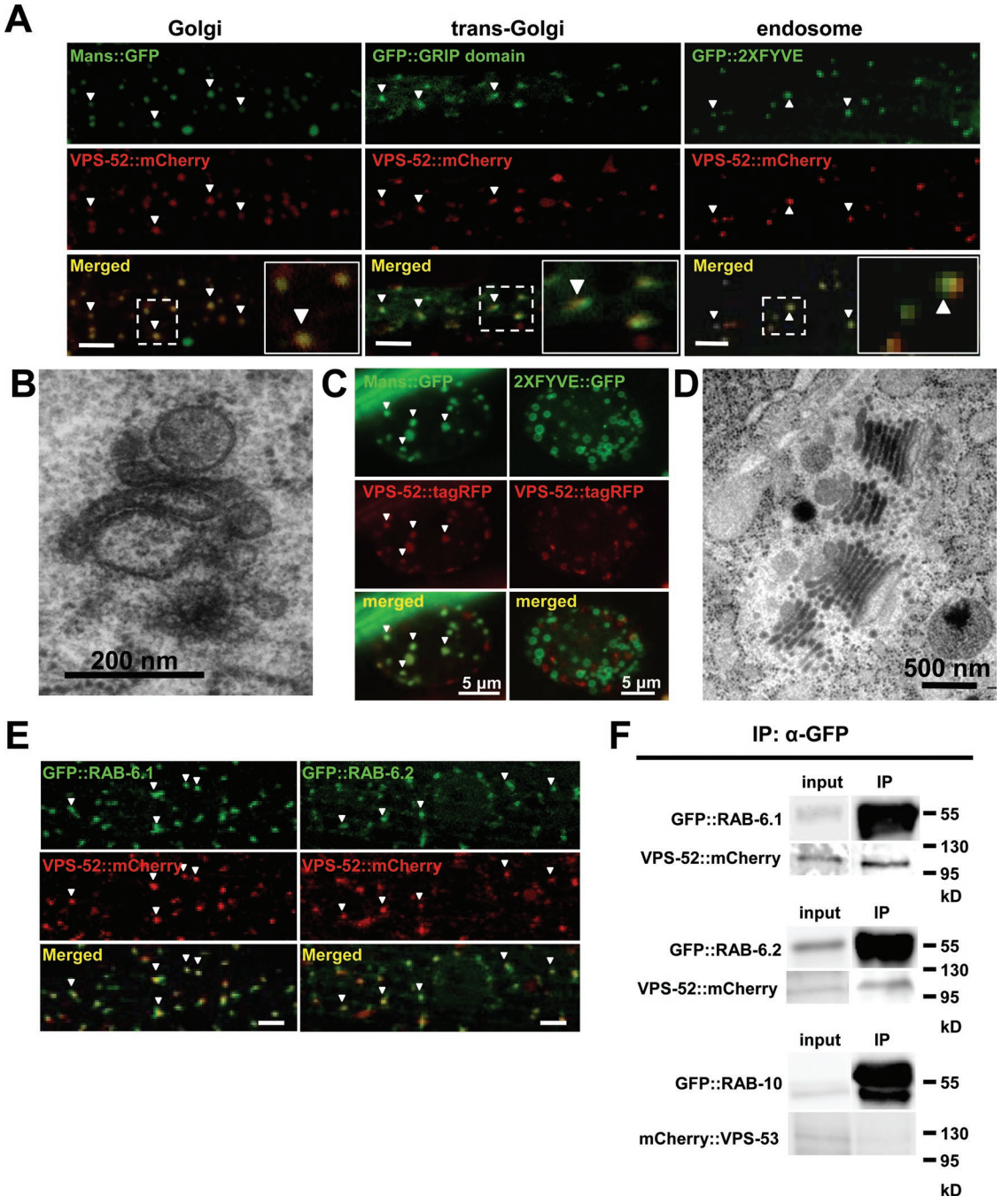

FIGURE 3: GARP complex localizes to the Golgi endosomal interface. (A) GARP complex localization overlaps with the medial Golgi (Mans::GFP) and late Golgi (GFP::GRIP domain) and partially with endosomal domains (GFP::2xFYVE) in body-wall muscles. Insets show magnifications of the marked regions of the merged fluorescence images. Scale bar, 5 µm. (B) Thin plastic section EM picture of a Golgi ministack present in *C. elegans* body-wall muscles. Scale bar, 200 nm. (C) GARP complex localization overlaps with the medial Golgi (Mans::GFP) but not with endosomal domains (2xFYVE::GFP) in coelomocytes. Scale bar, 5 µm. (D) Thin plastic section EM picture of Golgi stacks present in *C. elegans* coelomocytes. Scale bar, 500 nm. (E) VPS-52::mCherry can be colocalized with the *C. elegans* Rab6 orthologues GFP::RAB-6.1 and GFP::RAB-6.2. (F) VPS-52 can be coimmunoprecipitated with both Rab6 orthologues; GFP::RAB-10 was used as a negative control. Scale bar, 5 µm.

Loss of GARP activity leads to alterations in lysosomal morphology

To functionally characterize the GARP complex in a multicellular organism, we analyzed deletion mutant strains of each subunit in *C. elegans* (Figure 1A). Surprisingly, homozygous deletion mutants of each single GARP subunit were viable. However, mutants in the core subunits *vps-52*, *vps-53*, and *vps-54* had reduced brood sizes (*vps-52(ok853)*, 108 ± 7, N = 39; *vps-53(ok2864)*, 102 ± 12, N = 24; *vps-54(ok1463)*, 57 ± 5, N = 32) as compared with wild type (290 ± 7, N = 25). Because the brood size defects could be rescued by mating homozygous *vps-52* or *vps-54* mutant hermaphrodites with wild-type males, it is likely that mutations in the *C. elegans* GARP

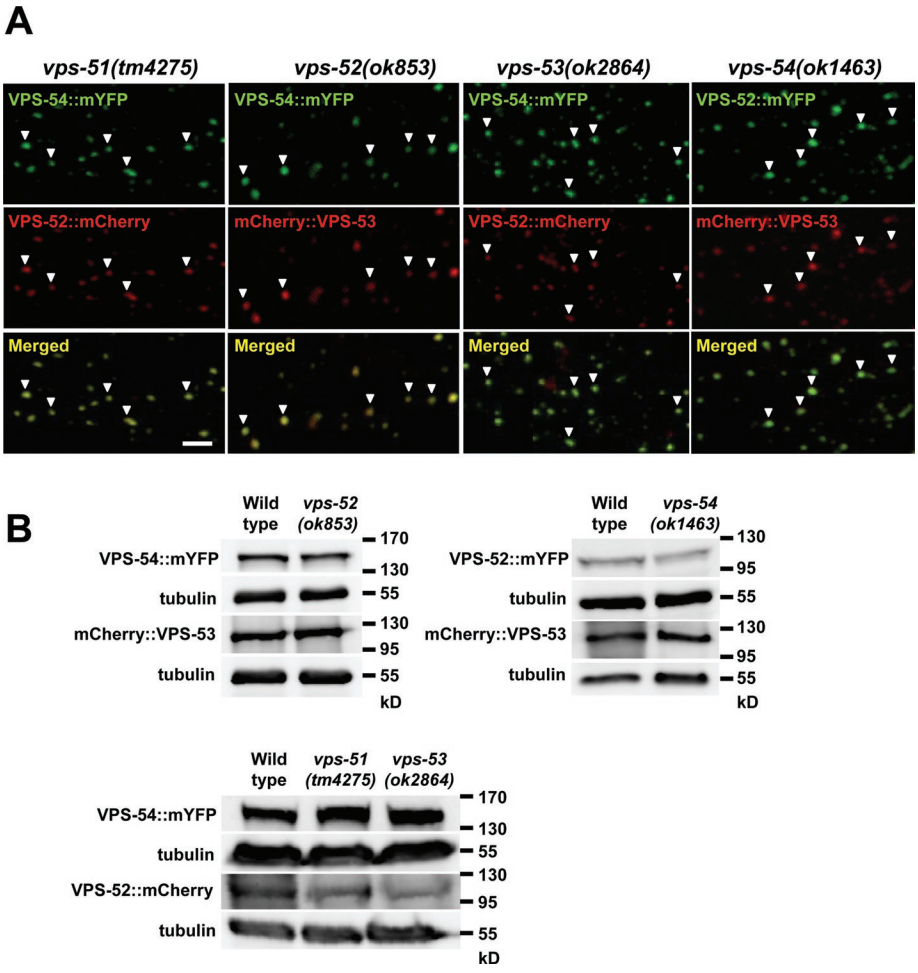

FIGURE 4: GARP subunit stability in mutant backgrounds. (A) Deletion of individual GARP subunits does not alter the localization of the rest of the complex in body-wall muscle cells. Scale bars, 5 μm. (B) Deletion of individual GARP subunits does not alter the stability of other subunits, as assayed by Western blotting.

complex lead to sperm defects as reported for mouse Vps54 mutants (Schmitt-John *et al.*, 2005). The brood size defect (198 ± 7, N = 25) is less severe in *vps-51(tm4275)* animals, suggesting that *C. elegans* VPS-51 might also be an auxiliary subunit of the GARP core complex as has been proposed in yeast (Siniossoglou and Pelham, 2002; Conibear *et al.*, 2003). In addition to their brood size defects, GARP mutant animals appeared slightly pale, grew more slowly than wild type, and displayed reduced locomotion (unpublished), although their morphological appearance was largely normal. Despite the loss of a particular GARP subunit, we could demonstrate that the remaining subunits were stable and still localized to the Golgi (Figure 4). Therefore it was possible that the remaining subunits could still support some GARP complex function sufficient to confer viability. To test this, we constructed double-mutant combinations of the different GARP subunits, which were all viable and phenotypically indistinguishable from the single-mutant animals (unpublished data). This suggests that in *C. elegans*, GARP complex function is not strictly required for viability. Thus it is likely that a redundant pathway exists that is able to compensate for the loss of GARP complex function.

To study how the loss of GARP complex function affects intracellular transport, we analyzed the effects of mutations in GARP complex subunits on the morphology of intracellular compartments. We chose to examine this in *C. elegans* coelomocytes, which are macrophage-like scavenger cells. They reside in the body cavity (pseudocoelom) and constantly filter the pseudocoelomic body fluid by bulk endocytosis. Coelomocytes are highly active in membrane transport and therefore are widely used to study endocytic membrane transport (Fares and Greenwald, 2001a, 2001b). Using transgenic marker strains, we did not observe any differences in structures of the secretory pathway such as the ER and Golgi complex, nor did we detect alterations in the early endocytic pathway (early and late endosomes) (Figure 5A). In contrast, we observed strongly enlarged lysosomal structures labeled by the transmembrane proteins CUP-5/mucolipin and LMP-1 (Fares and Greenwald, 2001b; Treusch *et al.*, 2004). In mutants of the GARP core complex, large vesicular structures positive for lysosomal markers with a diameter of more than 4 μm were detectable (Figure 5, A, B). These structures were already visible by differential interference contrast (DIC) microscopy (Figure 5C). We were not able to detect such enlarged lysosomes in the wild-type background. These enlarged lysosomal structures were similar in single- and double-mutant combinations of the GARP subunits (Figure 5A), suggesting that the single mutants correspond to a strong loss of GARP complex function.

An electron microscopic analysis revealed that these large structures are protein rich, as they are stained by osmium, like lysosomes (Figure 6). These large lysosomal structures were never detected in wild-type coelomocytes. In addition to the enlarged lysosomes, we also detected clear vacuolar structures that were enlarged in both *vps51(tm4275)* and *vps-52(ok853)* mutant backgrounds (Figure 6B, C). These clear vacuoles were generally surrounded by lysosomes and contained dark granular material inside. Although the identity of these structures is not clear, they may represent aberrant lysosomes or lipid-filled storage compartments. However, the uptake and transport kinetics of endocytosed material, such as Texas red–labeled bovine serum albumin (BSA) injected into the body cavity, was not affected in GARP mutant coelomocytes (Figure 7). Furthermore, in a separate assay for coelomocyte uptake, the fluorescence level of GFP that has been secreted into the body cavity and taken up by coelomocytes (Fares and Greenwald, 2001a) was similar between GARP mutants and wild type (Supplemental Figure S3B, C). This indicates that endocytosis is similar to that in wild type and suggests that lysosomal turnover of GFP is largely unaffected. To assay whether lysosomes are indeed fully functional in GARP mutants, we used the integrated marker strain *arIs36[phsp::ssGFP]*, which expresses secreted GFP (ssGFP) under the control of a heat shock–inducible promoter (Fares and Greenwald, 2001b). We crossed *arIs36[phsp::ssGFP]* into *vps-52(ok853)* mutants and induced the transient production of a pulse of ssGFP by a short heat shock. Subsequently, we followed the uptake of ssGFP into coelomocytes and its lysosomal degradation over time as described previously (Fares and Greenwald, 2001b). As expected from the previous experiments, the uptake of ssGFP in

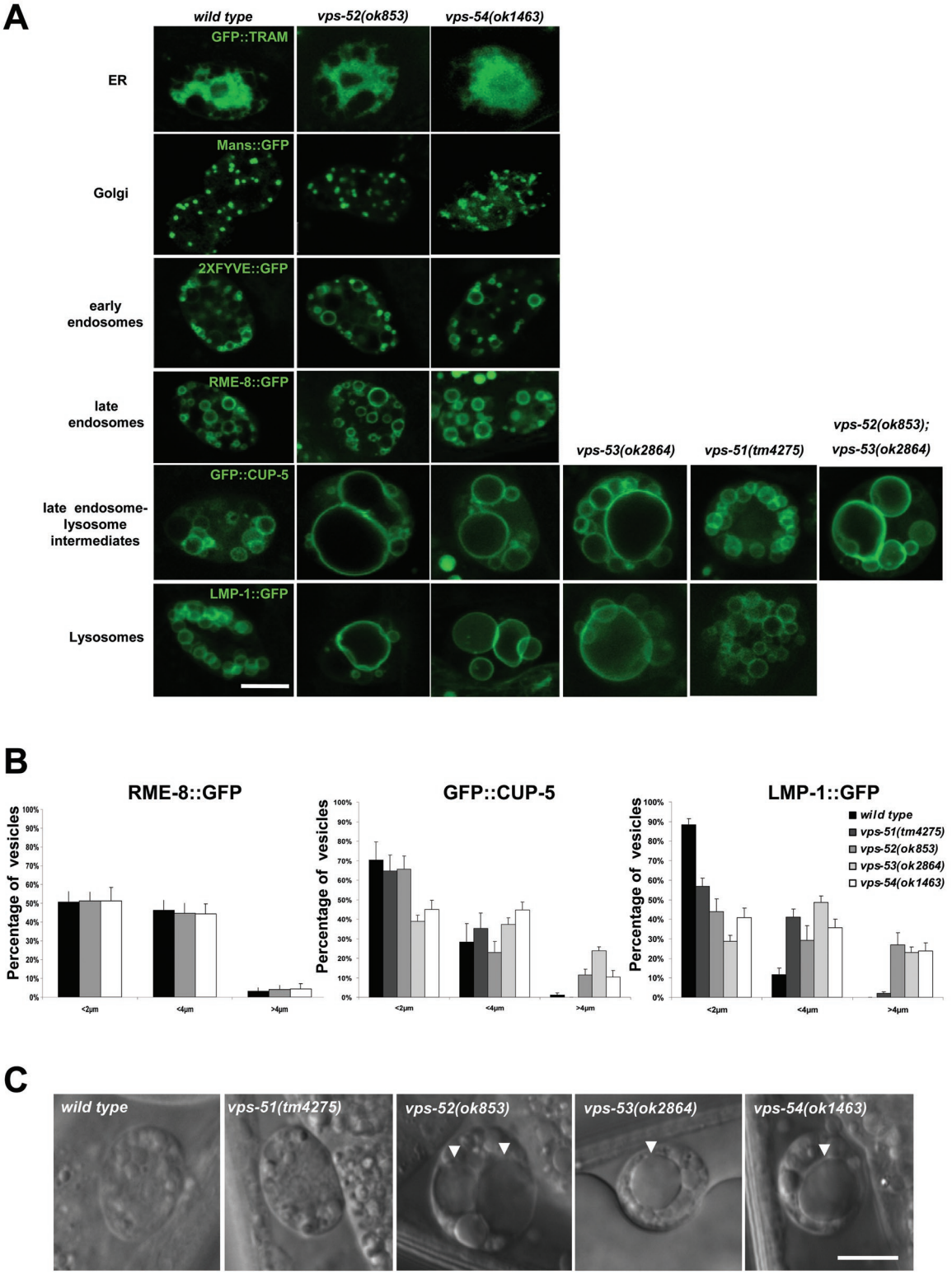

FIGURE 5: GARP complex mutations lead to enlarged lysosomes. (A) Confocal pictures of coelomocytes in which the indicated subcellular organelles are labeled. GARP mutants exhibit enlarged lysosomal structures. Scale bar, 5 μm. (B) Diameters of vesicles labeled by RME-8::GFP, GFP::CUP-5, and LMP-1::GFP in each coelomocyte were measured and divided into three categories: <2, 2–4, and >4 μm. The *y*-axis represents the percentage of each category. Error bars represent SEM. GARP mutants do not show a difference in the size of RME-8::GFP–labeled vesicles. *vps-52(ok853)*, *vps-53(ok2864)*, and *vps-54(ok1463)* mutants show a dramatic increase in the proportion of GFP::CUP-5 and LMP-1::GFP vesicles that are >4 μm. LMP-1::GFP vesicles in *vps-51(tm4275)* mutant show a decreased proportion in the category of <2 μm and an increased proportion in the category of 2–4 μm compared with wild type, although no significant change was seen in the category of >4 μm. (C) DIC pictures of coelomocytes. Enlarged vesicular structures (as indicated by arrow heads) are detectable in GARP mutants.

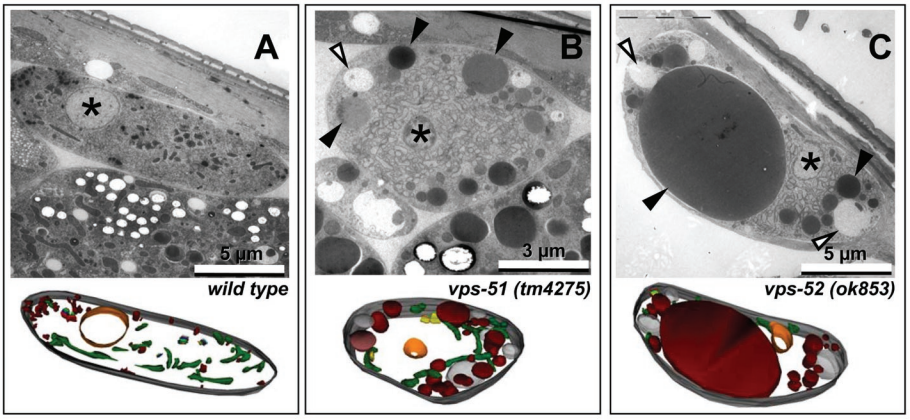

FIGURE 6: Serial EM reconstructions reveal enlarged compartments in GARP mutant coelomocytes. Electron microscopy images of 40-nm thin plastic sections of coelomocytes in wild type (A), *vps-51* (B), and *vps-52* (C) mutants are shown. Enlarged vesicular structures present in the GARP mutants are marked by arrowheads (filled for dark and open for clear vacuolar structures). The nucleus is marked with an asterisk. Bottom, serial reconstructions of 16 successive 40-nm thin sections per strain. Lysosomal compartments are labeled in brown, mitochondria in green, the nucleus in orange (marked with an asterisk), Golgi complexes as rainbow multicolored, and clear vacuolar structures present in the GARP mutants in gray.

vps-52 mutants followed the same kinetics as in the wild-type background (Supplemental Figure S4). It is striking that, roughly 26 h after the heat shock, wild-type and *vps-52* mutant coelomocytes had degraded comparable amounts of ssGFP (Supplemental Figure S4). Therefore lysosomes are likely functional in GARP mutants despite their morphological alterations.

VPS-51 is required for GARP complex function

Despite being an integral part of the GARP complex, *vps51* mutants in yeast display weaker growth defects than the other complex components. This is consistent with the fact that the core complex is still correctly assembled and localized in the absence of Vps51p (Siniossoglou and Pelham, 2002; Conibear *et al.*, 2003). This led to the idea that Vps51 might be an auxiliary GARP subunit. However, *vps51* mutants do show phenotypes similar to the rest of the GARP subunits. In yeast, Vps51p has been shown to affect the sorting of soluble vacuolar proteins and the recycling of the plasma membrane SNARE Snc1p. In addition, inactivation of Vps51p leads to fragmented vacuoles and defects in autophagosome formation similar to mutants in the other subunits (Siniossoglou and Pelham, 2002; Conibear *et al.*, 2003; Reggiori *et al.*, 2003). In the mammalian cells small interfering RNA–mediated knockdown of Vps51/Ang2 leads also to missorting of lysosomal enzymes, as well as impairment of protein retrieval to the TGN and autophagy (Perez-Victoria *et al.*, 2010). In *C. elegans*, *vps-51* mutants also show enlarged lysosomal structures, although these structures were mostly between 2 and 4 µm in size and never reached the size seen in the GARP core complex mutants (Figure 6C). Thus the VPS-51 subunit in *C. elegans* also contributes to basic GARP complex function. However, as in yeast, *vps-51* mutants may retain some GARP complex activity.

The GARP complex may support multiple retrograde routes to the Golgi through differential SNARE interactions

Yeast Vps51p was shown to bind to the late Golgi t-SNARE Tlg1p (Siniossoglou and Pelham, 2002; Conibear *et al.*, 2003). The mammalian Vps51/Ang2 has been demonstrated to bind to the regulatory Habc domain of the TGN SNARE syntaxin-6 (Perez-Victoria *et al.*, 2010). This led to the attractive model that the Vps51 subunit might be responsible for SNARE recruitment at the target membrane. The Tlg1 interaction motif was mapped to the very N-terminus of Vps51p (aa 18–30) and shown to form a short helix that interacts with a three-helix bundle formed by Tlg1p (Siniossoglou and Pelham, 2002; Fridmann-Sirkis *et al.*, 2006). Surprisingly, a deletion of the N-terminal domain of Vps51p or mutations that eliminate Tlg1p binding did not affect the ability of Vps51p to recycle proteins back to the Golgi. This led to the idea that the Vps51p/Tlg1p interaction may just increase the efficiency of the fusion reaction with the target membrane by ensuring the presence of all components required (Siniossoglou and Pelham, 2002; Conibear *et al.*, 2003; Fridmann-Sirkis *et al.*, 2006).

Recently, similar SNARE interactions have been demonstrated for the other GARP complex subunits. The mammalian GARP complex has been shown to directly bind late Golgi SNAREs syntaxin-6, -10, and -16, as well as VAMP4 (Liewen *et al.*, 2005; Perez-Victoria and Bonifacino, 2009; Perez-Victoria *et al.*, 2010). We therefore systematically tested the interactions of each complex subunit with almost all *C. elegans* SNARE proteins by yeast two-hybrid analysis (Figure 8A). VPS-54 interacted with the syntaxin-5 orthologue SYX-5 and the membrin/GS27 orthologue MEMB-2, which are both Golgi SNAREs. VPS-52 showed an additional binding to syntaxin-16 (SYX-16) present at the *trans*-Golgi and weak binding to the second *C. elegans* membrin orthologue, MEMB-1. VPS-51 interacted specifically with SYX-5 as well as with both MEMB-1 and MEMB-2. Furthermore, VPS-51 also binds the late Golgi SNAREs syntaxin-16 and the Vti1 orthologue, VTI-1 (Figure 8A), which has been shown to localize to the Golgi as well as to the Golgi endosomal interface. The SNARE interactions with VPS-53 could not be tested since it is autoactivating when fused to the DNA-binding domain within the yeast two-hybrid system. These results suggest that there are direct interactions of each GARP subunit with a specific set of Golgi SNAREs. To further support this finding, we labeled the GARP subunit VPS-53 with mCherry and analyzed its colocalization with GFP-tagged SNAREs that had been shown to interact with the different GARP subunits based on the yeast two-hybrid assays. When expressed under the control of the panneuronal *rab-3* promoter, the *trans*-Golgi SNAREs SYX-16 and VTI-1, as well as the earlier Golgi SNAREs SYX-5 and MEMB-2, showed colocalization with the mCherry-VPS-53 fusion protein in motoneurons (Figure 8B). This suggests that the GARP complex localizes to these SNARE domains.

Thus we wondered whether it would be possible to phenocopy the GARP complex mutant phenotype with respect to enlarged lysosomal structures by inactivating specific SNAREs. To address this, we used RNAi-mediated gene knockdown by bacterial feeding (Kamath *et al.*, 2001) of each SNARE individually in the RNAi-hypersensitive *eri-1* strain background expressing the lysosomal marker GFP-CUP-5. Of all SNARE molecules tested, knockdown of only the Golgi SNARE GOS28 (GOS-28) and the *trans*-Golgi SNARE syntaxin-6 (SYX-6) showed lysosomal structures larger than 4 µm at high frequency (Supplemental Figure S5). An intermediate lysosomal phenotype reminiscent of *vps-51* mutants was obtained with RNAi for Ykt6 (YKT-6) and Use1 (USE-1). Because RNAi against YKT-6 and USE-1 leads to slow growth, we cannot exclude that the observed

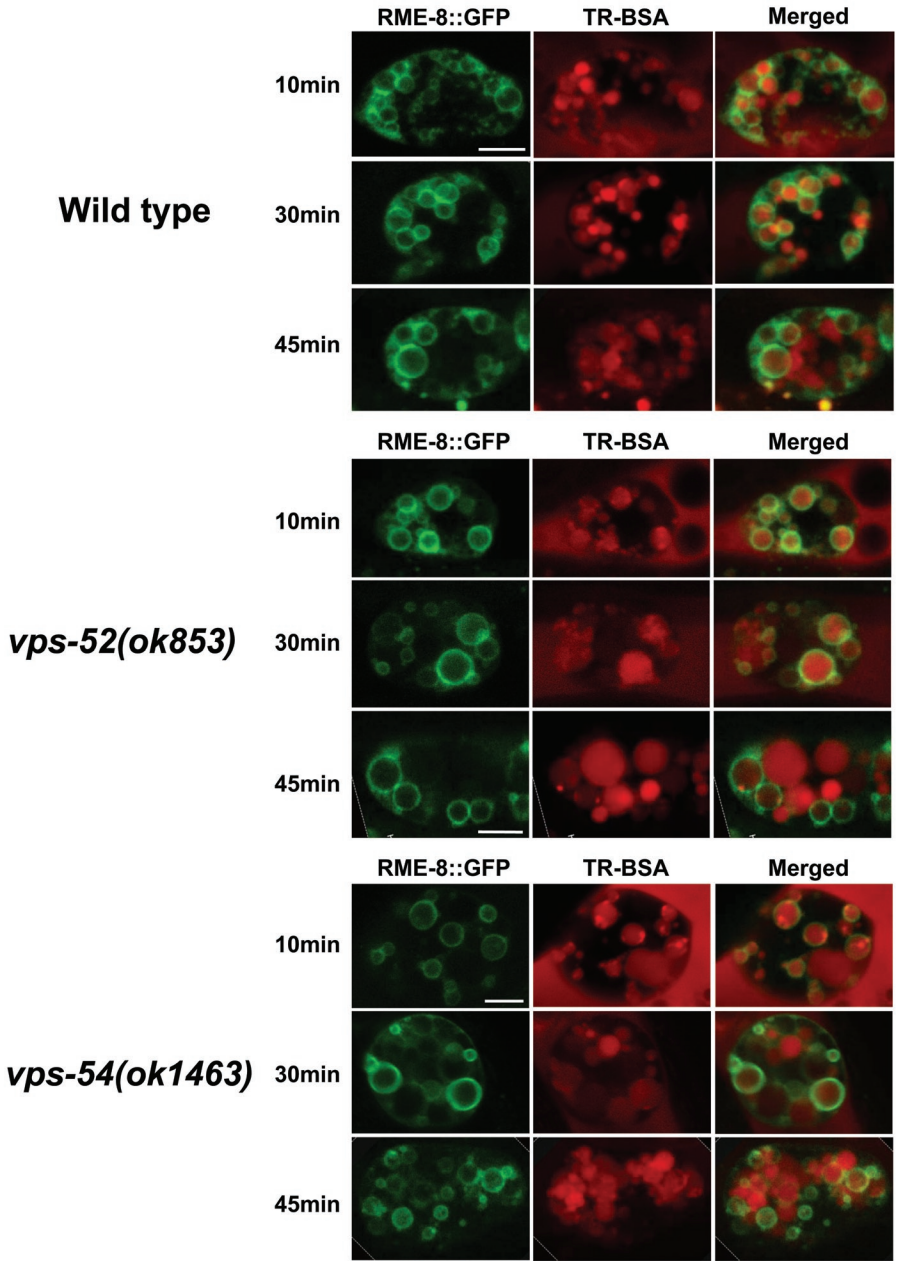

FIGURE 7: Coelomocyte endocytosis is not affected in GARP mutants. TR-BSA was microinjected into the body cavities of animals. Coelomocytes were tracked at indicated time spots by confocal microscopy. Late endosomes in coelomocytes were labeled by RME-8::GFP. Ten minutes after injection, TR-BSA had already entered the late endosomes. Thirty minutes after injection, part of the TR-BSA exited late endosomes and entered later structures, probably lysosomes. Forty-five minutes after injection, most of the TR-BSA exited late endosomes and entered later structures. No significant difference was seen in the endocytosis dynamics between wild type and GARP mutants. Scale bar, 5 μm.

size increase of lysosomal structures is due to a general sickness of the animals (see also Supplemental Table S1).

The interaction of the GARP subunits with specific SNARE molecules prompted us to analyze whether redundant or parallel SNARE pathways may exist that would compensate for the loss of GARP complex function. Routinely, this analysis is done best by screening for synthetic genetic interactions, which may lead to synthetic lethality. Screens for synthetic interactions between two factors can be assayed either by the construction of double-mutant animals or by RNAi-mediated inactivation of a particular gene in a mutant background. To increase RNAi efficiency, we used the RNAi-hypersensitive *eri-1(mg366)* mutant background (Lee *et al.*, 2006). Double mutants between *eri-1(mg366)* and *vps-52(ok853)* or *vps-54(ok1463)* were used to knock down each individual *C. elegans* SNARE, and the *eri-1* single mutant served as a control. As shown in Supplemental Table S1, we were unable to detect any synthetic sick or lethal interaction between the GARP subunits and SNARE molecules. Genetic interactions with *syx-5* and *nbet-1* could not be tested since RNAi against both SNAREs already causes lethality in the control strain. These experiments suggest that in the absence of GARP complex activity retrograde trafficking and tethering is functional enough to confer viability of the organism. This is most likely due to the fact that a redundant retrograde trafficking process exists that could compensate the loss of GARP complex function.

The COG tethering complex has also been shown to bind to the early Golgi SNARE Sed5/syntaxin-5 (Bruinsma *et al.*, 2004; Shestakova *et al.*, 2007). Therefore the COG and GARP complexes may be redundantly required for retrograde Golgi transport. *C. elegans* mutants in the COG subunits COGC-1 and -3 are viable and display only mild defects in gonad morphology (Kubota *et al.*, 2006). However, when *cogc-1(k179)* or *cogc-3(k181)* mutations were combined with a deletion of *vps-52*, a very strong synthetic lethality was observed (Figure 8C). The strength of the genetic interaction was even more impressive since both COG and GARP single-mutant animals were quite healthy. This suggests that COG and GARP complexes share overlapping functions for Golgi retrieval.

In summary, these results support a model in which the GARP tethering complex orchestrates retrograde transport to the Golgi through binding to multiple Golgi SNAREs.

DISCUSSION

As in yeast, GARP complex–mediated Golgi retrieval is not required for viability in *C. elegans*. In contrast, *Vps54*-null mutations in the mouse lead to embryonic lethality, most likely due to cardiovascular malfunction (Schmitt-John *et al.*, 2005). In addition, homozygous *Vps54*$^{-/-}$ mice showed abnormalities in spinal cord development and a lack of dorsal root ganglia, suggesting that GARP function is required for the generation of specific higher-order structures during vertebrate development. Common features of GARP complex mutants in all multicellular systems are male-specific defects in either sperm development, as in mice and in *C. elegans* (as shown here; also see Schmitt-John *et al.*, 2005), or pollen development, as reported for *Arabidopsis* (Guermonprez *et al.*, 2008). This further suggests

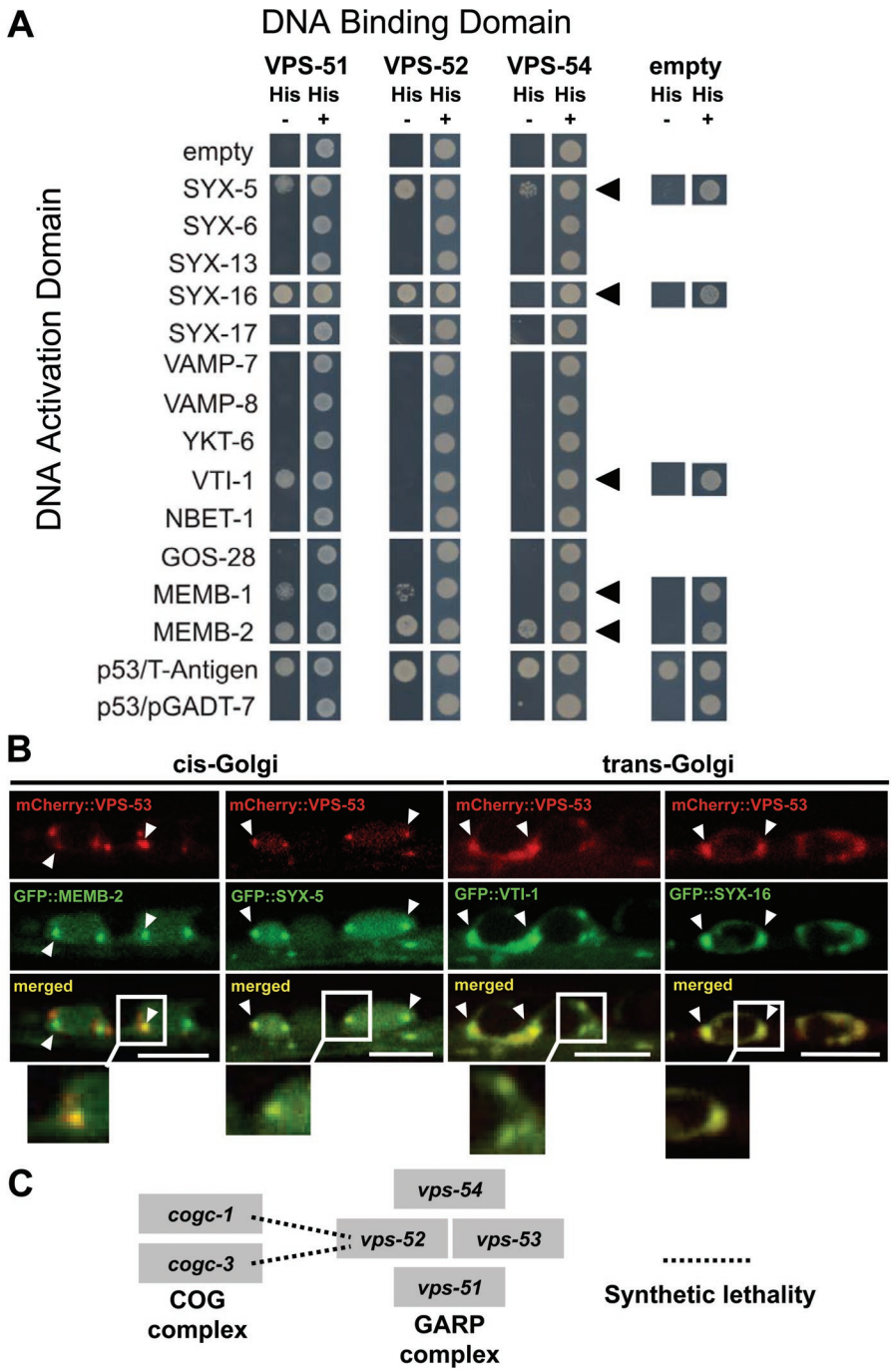

FIGURE 8: GARP complex interacts with early and late Golgi SNAREs. (A) Interactions of GARP subunits with Golgi and endosomal SNAREs were assayed by yeast two-hybrid analysis. The growth medium without histidine selects for interactions. (B) mCherry::VPS-53 colocalizes with GFP::MEMB-2, GFP::syntaxin-5, GFP::VTI-1, and GFP::syntaxin-16 in motoneurons. Insets show magnified parts of the pictures. Scale bar, 5 μm. (C) The GARP complex shows a genetic interaction with the COG complex. The *vps-52(ok853)* mutant is synthetically lethal with the available *cogc-1(k179)* and *cogc-3(k181)* mutants, which encode subunits of the COG complex.

that GARP activity is particularly required for very specialized membrane trafficking events during spermatogenesis. The fact that GARP complex activity is not required for basal cell survival or the development of yeast and *C. elegans* may point to parallel and partially redundant Golgi retrieval pathways. Here we show that COG complex–mediated retrieval pathways might be able to partially compensate for the lack of GARP complex activity, since loss of both GARP and COG complexes leads to synthetic lethality in *C. elegans*. Thus most of the cargo that has to be retrieved back to the Golgi may either be able to use both COG- and GARP-dependent retrieval pathways at steady state or might be able to switch retrieval routes if one pathway is compromised. Additional evidence for a parallel or overlapping function of GARP and COG retrograde tethering complexes comes from our observation that some of the *C. elegans* GARP subunits interact with the Golgi SNARE syntaxin-5 within the yeast two-hybrid system (Figure 8A). The COG complex has previously been shown to bind syntaxin-5/Sed5p in mammals and yeast and has been demonstrated to support tethering to the early Golgi (Bruinsma *et al.*, 2004; Shestakova *et al.*, 2007; Smith *et al.*, 2009), partly also through its interaction with the SM protein Sly1 (Koumandou *et al.*, 2007; Laufman *et al.*, 2009). Thus the GARP complex might use multiple tethering modes to the Golgi, some of which might also be supported by the COG complex. This has also been suggested by the finding that specific mutations in *VPS53* in yeast can be suppressed by the dominant SLY1 allele *SLY1-20* (Vanrheenen *et al.*, 2001), which is also able to suppress mutations in the COG complex components *SEC34* and *SEC35* (VanRheenen *et al.*, 1998, 1999). This observation led the authors suggest that Vps53p may also have some function at the *cis*-Golgi, in addition to its reported role at the *trans*-Golgi together with the SNARE Tlg1p (Conibear and Stevens, 2000; Siniossoglou and Pelham, 2002; Conibear *et al.*, 2003). In contrast to earlier reports, which implicated syntaxin-5/Sed5p mainly in trafficking at the *cis*-Golgi side, it was subsequently found that syntaxin-5 and its SNARE complex partners are distributed widely across the Golgi stacks, consistent with a function at later Golgi stages (Hay *et al.*, 1998; Orci *et al.*, 2000; Volchuk *et al.*, 2004). Of interest, a syntaxin-5–containing SNARE complex has recently also been implicated in early/recycling endosome to *trans*-Golgi transport. Specific depletion of syntaxin-5 dramatically reduced the retrograde transport of bacterial Shiga toxin B (STxB) subunit to the *trans*-Golgi (Tai *et al.*, 2004; Amessou *et al.*, 2007). Furthermore, the effects of syntaxin-5 were similar to the down-regulation of *trans*-Golgi SNARE syntaxin-16, which has been demonstrated to be required for early endosome to Golgi trafficking (Mallard *et al.*, 2002). Strikingly, inhibition of syntaxin-5 or syntaxin-16 showed the same kinetics of STxB transport inhibition. Because both SNAREs are part of distinct functional complexes, this has led to the notion that a syntaxin-16– as well as a

syntaxin-5–dependent retrieval pathway to the *trans*-Golgi may exist (Tai *et al*., 2004).

However, COG and GARP complexes also supply clearly distinct and nonoverlapping functions for intracellular trafficking. It has been reported that loss of COG complex activity in *C. elegans* leads to distal tip cell (DTC) migration defects, resulting in aberrant gonad morphology (Kubota *et al*., 2006). In contrast, DTC migration defects were not observed in GARP complex mutants (L.L. and S.E., unpublished data). These defects have been shown to be caused mainly by the lack of glycosylation of the secreted metalloprotease MIG-17, which subsequently fails to localize to the gonadal basement, where it is required for proper DTC migration (Kubota *et al*., 2006). On the basis of wheat germ agglutinin staining of mutant extracts, COG mutations seem to cause a general hypoglycosylation of protein within the secretory apparatus, most likely due to mislocalization of Golgi-resident glycosyltransferases, as in mammals (Ungar *et al*., 2006; Smith and Lupashin, 2008). Similar glycosylation defects could not be detected in mutants of the *C. elegans* GARP complex (L.L. and S.E., unpublished data). This suggests that each tethering complex also has specialized or additional functions, which are not shared by the other retrieval pathway. Thus the trafficking of some of the cargo might depend on a particular pathway.

In yeast, mutations in the GARP core complex *vps52/vps53/vps54* also lead to alterations in lysosomal morphology, causing lysosomal fragmentation (Conboy and Cyert, 2000; Conibear and Stevens, 2000; Siniossoglou and Pelham, 2001, 2002). In contrast, mutations in the *C. elegans* GARP core complex lead to strongly enlarged lysosomes. A similar lysosomal phenotype has been observed in mutants of the *C. elegans* PIKfyve/Fab1p phosphoinositide kinase PPK-3, which phosphorylates phosphatidylinositol-3-monophosphate into phosphatidylinositol-3,5-bisphosphate (Nicot *et al*., 2006). Thus the localization or function of this phosphatidylinositol-3-phosphate-5-kinase may depend on GARP-dependent retrograde trafficking.

In addition, inefficient retrieval from endosomal compartments in GARP complex mutants may cause an increase of cargo and membrane flow into the endosomal–lysosomal pathway. The lysosome, as terminal compartment, might be the last acceptor of this increased flow and thus has to adapt by enlargement. On the basis of pulse-chase experiments we can demonstrate that these enlarged lysosomal structures are still functional and degrade endocytosed GFP with kinetics similar to those of wild type (Supplemental Figure S4). A morphological analysis of GARP mutant coelomocytes by electron microscopy (EM) further revealed that in addition to enlarged lysosomes, enlarged clear vesicular structures were also detectable (Figure 6). These clear vesicular structures often contained darker inclusions. At this point we do not know to what these clear structures correspond, but they may resemble aberrant lysosomes or lipid-rich storage compartments. Knockdown of Vps51/Ang2 in mammalian cells has been shown to cause not only mistargeting of lysosomal hydrolases, but also a proliferation of lysosomal structures to larger vacuoles that were often filled with membranous material (Perez-Victoria *et al*., 2010). In contrast to *C. elegans* coelomocytes, these lysosomes have been report to exhibit impaired lysosomal proteolysis.

In *C. elegans*, enlarged lysosomes similar to GARP mutants could also be induced specifically by RNAi-mediated knockdown of the SNAREs GOS-28, syntaxin-6/SYX-6, YKT-6, and USE-1 (Supplemental Figure S5). Of interest, most of these SNAREs have been linked to retrograde trafficking within the Golgi, endosome to Golgi, and Golgi to ER (Lupashin *et al*., 1997; Dilcher *et al*., 2001, 2003; Tai *et al*., 2004; Volchuk *et al*., 2004; Maekawa *et al*., 2009). This further supports the view that inefficient retrieval at Golgi and endosomal domains leads to a strongly increased flow of membranes and cargo to the lysosomal compartment and thus enlargement. It is interesting to note that the SNAREs that lead to lysosomal enlargements in the RNAi experiment match very well with the SNAREs that have been found to interact with the GARP subunits within the yeast two-hybrid system (Figure 8A). Gos28 and Ykt6 have been reported to be in a specific complex with GS15 and syntaxin-5, and the latter also binds to the GARP complex subunits (Tai *et al*., 2004). This specific SNARE complex has been shown to be required for retrograde transport within the Golgi and from endosome to Golgi (Tai *et al*., 2004). In *C. elegans* GOS-28 has also been reported to display synthetic lethality when YKT-6 is knocked down by RNAi in a *gos-28* mutant background (Maekawa *et al*., 2009). The same authors also noted that *gos-28* displays in addition synthetic interactions with COG complex components and syntaxin-5/SYX-5. In addition, a separate SNARE complex consisting of Sed5/Vti1/Sft1/Ykt6 has also been reported in yeast to mediate vesicular transport from the prevacuolar compartment to the early Golgi (Fischer von Mollard and Stevens, 1999) in a Ypt6/Rab6–dependent manner (Bensen *et al*., 2001). However, additional possible Sed5p-containing SNARE complexes have been described in vitro (Tsui *et al*., 2001). We also identified syntaxin-6 by RNAi and syntaxin-16/SYX-16 and VTI-1 in the two-hybrid assay as binding partners of the GARP subunits VPS51 and VPS-52 in *C. elegans* (Figure 8A and Supplemental Figure S5). In the mammalian system syntaxin-6 is found in a complex with syntaxin-16 and Vti1, which localize to the late Golgi/TGN and form a SNARE complex with VAMP4 (Jahn and Scheller, 2006). The corresponding yeast SNARE complex is composed of Tlg2p/Vti1p/Tlg1p/Snc1/2p (Burri and Lithgow, 2004). Both syntaxin-6 and its corresponding yeast orthologue Tlg1p have been reported to bind to the GARP complex (Siniossoglou and Pelham, 2002; Conibear *et al*., 2003; Fridmann-Sirkis *et al*., 2006; Perez-Victoria and Bonifacino, 2009; Perez-Victoria *et al*., 2010). Thus, given that a great deal of redundancy and promiscuity has been documented in the SNARE system (Tsui and Banfield, 2000), tethering complexes may help to match the right combination of various SNARE molecules. The GARP complex might achieve this by preassembling SNAREs in a fusion-competent state through interactions with multiple SNARE molecules. Our observation that the GARP complex may interact with different sets of specific SNARE pairs further suggests that it may support multiple routes to different Golgi domains. Some of these routes might partially overlap or also be supported by other tethering complexes like the COG complex.

What is the function of VPS-51?

We showed that the *C. elegans* GARP complex also contains the Vps51 subunit originally identified in yeast. Furthermore, we demonstrate that Vps51 is evolutionarily conserved and that metazoan Vps51 is larger (≥700 aa) than the yeast counterpart (~150 aa). The VPS-51 subunit is tightly bound to the other GARP subunits and can be coimmunoprecipitated with the core complex. Yeast Yps51p has been reported to bind to the late Golgi SNARE Tlg1p (Siniossoglou and Pelham, 2002; Conibear *et al*., 2003), whereas the mammalian Vps51 subunit was found to interact with the regulatory Habc domain of sytaxin-6 (Perez-Victoria *et al*., 2010). Thus Vps51p was considered to serve as a specific adaptor that links the GARP core complex to the SNARE machinery at the acceptor membrane. This was an attractive model since it points to a mechanism by which the GARP complex would support SNARE pairing at the acceptor membrane. Subsequently, however, it was shown that mammalian GARP core complex subunits also bind to several late Golgi SNAREs and

that SNARE-binding domains could be localized on all GARP subunits (Liewen *et al.*, 2005; Perez-Victoria and Bonifacino, 2009; Perez-Victoria *et al.*, 2010). In *C. elegans*, we confirmed that all GARP subunits analyzed bind to a specific set of SNAREs. This may suggest that the SNARE-binding activity of the Vps51 subunit might not be its main activity. The fact that *vps51* mutants in yeast and *C. elegans* display weaker phenotypes may suggest that Vps51 subunits are essential for more specialized functions of the GARP complex. In agreement with this, the zebrafish Vps51 orthologue *ffr* has been shown to regulate fat metabolism (Farber *et al.*, 2001; Ho *et al.*, 2006). *fat-free* mutant fish embryos display lipid processing defects in the pancreas and vesicular recycling defects in the intestine, as well as degeneration of biliary epithelial cells and dilated Golgi structures within the digestive tract. However, the growth and morphology of *ffr* mutant fish were normal (Ho *et al.*, 2006). In the mammalian system, Vps51/Ang2, together with the other GARP subunits, has been shown necessary for protein retrieval to the TGN and sorting of lysosomal hydrolases but also to be required for proper autophagy (Perez-Victoria *et al.*, 2010), which may be a consequence of reduced lysosomal function. These results indeed suggest that Vps51 may serve as an adaptor for the GARP complex that has adopted specific functions in multicellular systems. These functions might have been dispensable in yeast, and thus yeast Vps51 was subsequently shortened to a minimal unit. Thus these findings may provide a framework that will lead to a more detailed view of the tethering reaction mediated by the GARP complex at the acceptor membranes of the Golgi.

MATERIALS AND METHODS

Strains

Strains were maintained at 20°C and cultured as previously described (Brenner, 1974). Strains used in this study were as follows: Bristol N2 wild-type strain, *vps-51(tm4275)* I, *vps-52(ok853)* X, *vps-53(ok2864)* III, *vps-54(ok1463)* V, *vps-35(hu68)* II, *pwIs50[lmp-1::GFP + unc-119(+)]*, *bIs1[vit-2::GFP]* X, *bIs34[rme-8::GFP]*, *cdIs40[pcc1::GFP::CUP-5]*, *cdIs54-[pcc1::MANS::GFP]*, *cdIs29[pcc1::GFP::TRAM]*, *cdIs85[pcc1::2x-FYVE::GFP]*, *rab-6.2(ok2254)* X, *cogc-1(k179)* I, *cogc-3(k181)* I, *arIs37[pmyo-3::ssGFP]* I, *arIs36[phsp::ssGFP]*, *eri-1(mg366)*. All strains were outcrossed at least three times before analysis.

DNA constructs and the generation of transgenic animals

vps-51/B0414.8, *vps-52/F08C6.3*, *vps-53/T05G5.8*, and *vps-54/T21C9.2* cDNAs were PCR amplified from a *C. elegans* mixed-stage cDNA library (Proquest; Invitrogen, Carlsbad, CA), subcloned, and verified by sequencing. Except for *vps-52*, all cDNAs were shown to be according to the WormBase predictions (www.wormbase.org). The corrected VPS-52 sequences have been submitted to GenBank (HQ237455). To express the different GARP complex subunits in *C. elegans* body-wall muscle cells under the control of the *myo-3* promoter, the respective cDNA along with a fluorescent protein tag was cloned into pPD115.62(*pmyo-3::gfp*), replacing GFP. As fluorescent protein tag, mYFP citrine, mCherry, or tagRFP (Evrogen, Moscow, Russia) was used. *vps-51* and *vps-53* were N-terminally tagged, and *vps-52* and *vps-54* were tagged at the C-terminus. To examine the subcellular localization of VPS-52 in coelomocytes, a construct that expresses a translation fusion of tagRFP to the C-terminus of VPS-52 under the control of the *vps-52* promoter (470 base pairs) was used. This construct was injected into the strains *cdIs54[pcc1::MANS::GFP]* and *cdIs85[pcc1::2xFYVE::GFP]* carrying integrated arrays that label Golgi and early endosomal structures in coelomocytes.

To analyze the expression pattern of *vps-51* and *vps-52* a 3.6-kb, 470–base pair promoter fragment upstream of the start ATG, respectively, was amplified from genomic DNA and subcloned as a *Hin*dIII and *Bam*HI fragment into *pPD115.62* (*pmyo-3::gfp*) by replacing the *myo-3* promoter. In the case of the *vps-53* promoter, a 4.5-kb promoter fragment was used starting at the ATG of the upstream gene (T05G5.9) of the *vps-53* operon. All clones were verified by sequencing.

To analyze SNARE proteins that may potentially genetically interact with the GARP complex, we amplified *memb-1/B0272.2*, *memb-2/M03E7.5*, *gos-28/F08F8.8*, *syx-5/F55A11.2*, *syx-6/C15C7.1*, *syx-7/F36F2.4*, *syx-16/ZC155.5*, *syx-17/VF39H2L.1*, *vamp-7/Y69A2AR.6*, *vamp-8/*B0513.9, *vti-1/Y57G11C.4*, *nbet-1/Y59E9AL.7*, *ykt-6/B0361.10*, *use-1/Y110A7A.11*, *sec-20/F40G9.1*, and *sec-22/F55A4.1* by PCR from a *C. elegans* mixed-stage cDNA library (Proquest; Invitrogen) and subcloned them into L4440 RNAi vector (Kamath *et al.*, 2001). To examine whether some SNARE proteins (VTI-1, syntaxin-5, syntaxin-16, and MEMB-2) colocalize with the GARP complex in neurons, we subcloned respective cDNA with a GFP tag at their N-terminals under the control of the panneuronal *rab-3* promoter.

To generate transgenic animals, young adult hermaphrodites were used for microinjection of DNA mixes into the distal part of the gonads (Mello *et al.*, 1991). Expression constructs were injected at 20 ng/µl and protein fusions at 5 ng/µl. *pttx-3::gfp* and *rol-6 (su1006)* were used as coinjection markers each at 30 ng/µl. The total DNA concentration of injection mixtures was adjusted to 120 ng/µl by adding *pBlueScript SKII* (Stratagene, Santa Clara, CA).

Coimmunoprecipitation and Western blotting

C. elegans mixed-staged worms from two 9-cm nematode growth medium (NGM) plates were rinsed off, washed, and snap frozen in liquid nitrogen and kept at −80°C until subsequent use. The frozen worm pellet was ground with a mortar and pestle and frozen in liquid nitrogen. While it was thawing, four to five volumes of homogenization buffer (50 mM HEPES, 7.5% glycerol, 10 mM NaCl, 1 mM EDTA, 0.1% NP-40) and complete EDTA-free protease inhibitor (Roche, Indianapolis, IN) were added. The suspension was kept at 4°C and centrifuged at 500 × *g* for 10 min. A total of 1.5 ml of supernatant was incubated with 4 µg of monoclonal mouse anti-GFP (Invitrogen) for 3 h at 4°C. A 10-µl amount of protein A–coated paramagnetic beads slurry (New England Biolabs, Ipswich, MA) was added and incubated for 2 h at 4°C. Beads were washed three times with 1 ml of homogenization buffer and eluted by adding 2× Laemmli buffer at 96°C. Western blotting was done according to the standard method. To detect mCherry fusion proteins, a polyclonal rabbit anti-DsRed (Clontech, Mountain View, Ca) was used at 1:1000 dilution. Secondary horseradish peroxidase–labeled anti–mouse and anti–rabbit antibodies were purchased from Jackson/Dianova (Hamburg, Germany) and used at 1:10,000.

Phylogenetic analysis

Phylogenetic trees were generated based on the PFAM Vps51 (PF08700) full alignment and subsets thereof, respectively, of full-length sequences selected based on phylogeny and aligned using MAFFT (Katoh *et al.*, 2005). Trees were constructed using neighbor joining (Howe *et al.*, 2002; Frickenhaus and Beszteri, 2008) and Bayesian inference (Ronquist and Huelsenbeck, 2003). Motif discovery was carried out using MEME (Bailey *et al.*, 2009). A detailed analysis is described in the Supplemental Material.

Coelomocyte and oocyte uptake assays

Pulse-chase assays were done by injecting 1 mg/ml Texas red (TR)–BSA into the pseudocoelom of young adult hermaphrodites as described (Treusch *et al.*, 2004). After recovery on NGM plates at 20°C

for 10, 30, and 45 min, worms were mounted, and the coelomocytes were imaged by confocal microscopy.

Pulse-case analysis of coelomocyte function by heat-shock induced expression of ssGFP was carried out as previously described (Fares and Greenwald, 2001b). Worm strains containing the integrated *arIs36[phsp::ssGFP]* array, which allows heat shock–induced expression of ssGFP, were grown at 20°C and synchronized at the L4 stage. The L4 larvae were heat shocked at 33°C for 30 min and returned to 20°C. The coelomocytes were imaged by confocal microscopy using the same parameter setting at 3.5, 6, and 26 h after the heat shock, respectively.

To analyze the uptake of the secreted yolk protein VIT-2-GFP fusion into oocytes, the integrated marker array *bIs1[vit-2::GFP]* was crossed into *vps-52(ok853)*, and *vps-54(ok1463)* mutants and proximal oocytes were subsequently imaged by confocal microscopy as described (Grant and Hirsh, 1999).

Confocal microscopy and data analysis

Transgenic worms were paralyzed by 50 mM sodium azide and mounted on 2% agarose pads. Confocal images were taken using a Leica SP2 inverted confocal microscope equipped with 488- and 561-nm laser diodes. The intensity and size of vesicular structures in coelomocytes were normalized to the background and quantified by using ImageJ.

Electron microscopy

A 100-μm-deep aluminum platelet (Microscopy Services, Flintbek, Germany) was filled with *Escherichia coli* OP 50 suspension. About 20 young adult worms were transferred into the chamber and immediately high-pressure frozen using a BalTec HPM 10. Freeze substitution was carried out in a Leica EM AFS at −90°C for 100 h in 0.1% tannic acid and another 7 h in 2% OsO_4 (each wt/vol in dry acetone), as described (Rostaing *et al.*, 2004).

A Leica UC6 ultramicrotome was used to cut 40-nm sections, and ribbons of serial sections were transferred on Formvar-coated copper slot-grids. The grids were stained with 4% (wt/vol) uranyl acetate in 75% methanol and analyzed using a Zeiss EM 902A TEM with a 1024 × 1024 charge-coupled device detector (Proscan Electronic Systems, Scheuring, Germany).

Three-dimensional images of coelomocytes were reconstructed from serial 40-nm thin plastic EM sections. Consecutive images of serial sections were imported into the "reconstruct" program (Fiala, 2005) and aligned linearly by setting traces. All structures (nucleus, mitochondria, Golgi stacks, and further cell inclusions) were surrounded on each image as closed structure and reconstructed as "Boissonnat surface" at 32 facets.

Yeast two-hybrid assay

The Matchmaker yeast two-hybrid assay was performed according to the manufacturer's protocol (Clontech). *vps-51*, *-52*, *-53*, and *-54* were cloned into the bait vector pGBKT7 (Clontech) as well as in the prey vectors pGADT7 (Clontech). All *C. elegans* SNARE proteins were identified and annotated by sequence comparison (Kloepper *et al.*, 2008), and the respective cDNAs were PCR amplified and subcloned into pGBKT7 as well as pGADT7. The appropriate plasmid combinations were transformed into the yeast strain AH109 (Clontech). Yeast transformants were spread onto growth media lacking leucine and tryptophan for plasmid selection. Interactions were tested as follows: several clones of transformants were mixed, diluted to OD_{600} of 0.2, and spotted onto selective plates lacking leucine, tryptophan, and histidine. Interactions were identified by growth after 3–4 d at 30°C. All interacting proteins were tested for self-activation as described earlier, using the appropriate empty vector pGBKT7 or pGADT7, respectively.

RNA interference experiments

Constructs that contain SNARE cDNAs in the L4440 RNAi vectors were transformed into the *E. coli* HT115 (DE3) strain that has been used for RNAi induced by bacterial feeding (Kamath *et al.*, 2001). After transformation, plasmid-containing HT115 (DE3) bacteria were inoculated in LB medium containing 100 μg/ml ampicillin, grown to OD_{600} = 1, and seeded onto 3.5-cm NGM plates supplemented with 1 mM isopropyl β-D-1-thiogalactopyranoside and 100 μg/ml ampicillin. From 10 to 15 young adult hermaphrodites were placed on each RNAi plate and transferred to a new plate every day. To score the RNAi phenotype, young adult F1 progeny were analyzed and imaged by confocal microscopy. To increase the efficiency of RNAi, the RNAi-hypersensitive *eri-1(mg366)* strain background was used (Lee *et al.*, 2006). For an unknown reason, in our hands RNAi bacteria transformed with the *syx-16*-RNAi vector grew extremely slowly and thus were omitted from further analysis. In the case of *syx-5* and *nbet-1* RNAi, which lead to mostly embryonic or larval lethality animals, we analyzed animals that escaped the lethality and grew to adulthood.

ACKNOWLEDGMENTS

We thank the *C. elegans* knockout consortia in Oklahoma, Vancouver, and Japan for providing the deletion mutants; Christian Olendrowitz for help with the statistical analysis; and the lab of S. Eimer for comments. This research was supported in part by the Max Planck Society and by the Deutsche Forschungsgemeinschaft Heisenberg Scholarship Z.W. 71/2-1 and 3-1 to M.Z. L.L. was supported by Neuroscience Early Stage Training program funded by the European Commission Frame Work Program 6, N.S. by a Ph.D. fellowship from the Göttingen Graduate School for Neurosciences and Molecular Biosciences, and M.A. by a postdoctoral fellowship from the Helen Hay Whitney Foundation and by National Institutes of Health Grant K99 MH082109. The European Neuroscience Institute Göttingen is jointly funded by the University Medical Faculty Göttingen and the Max-Planck Society. This work was further supported by the European Union coordination action Network of European Neuroscience Institutes.

REFERENCES

Amessou M, Fradagrada A, Falguieres T, Lord JM, Smith DC, Roberts LM, Lamaze C, Johannes L (2007). Syntaxin 16 and syntaxin 5 are required for efficient retrograde transport of several exogenous and endogenous cargo proteins. J Cell Sci 120, 1457–1468.

Bailey TL, Boden M, Buske FA, Frith M, Grant CE, Clementi L, Ren J, Li WW, Noble WS (2009). MEME SUITE: tools for motif discovery and searching. Nucleic Acids Res 37, W202–W208.

Bensen ES, Yeung BG, Payne GS (2001). Ric1p and the Ypt6p GTPase function in a common pathway required for localization of trans-Golgi network membrane proteins. Mol Biol Cell 12, 13–26.

Brenner S (1974). The genetics of *Caenorhabditis elegans*. Genetics 77, 71–94.

Bruinsma P, Spelbrink RG, Nothwehr SF (2004). Retrograde transport of the mannosyltransferase Och1p to the early Golgi requires a component of the COG transport complex. J Biol Chem 279, 39814–39823.

Burri L, Lithgow T (2004). A complete set of SNAREs in yeast. Traffic 5, 45–52.

Conboy MJ, Cyert MS (2000). Luv1p/Rki1p/Tcs3p/Vps54p, a yeast protein that localizes to the late Golgi and early endosome, is required for normal vacuolar morphology. Mol Biol Cell 11, 2429–2443.

Conibear E, Cleck JN, Stevens TH (2003). Vps51p mediates the association of the GARP (Vps52/53/54) complex with the late Golgi t-SNARE Tlg1p. Mol Biol Cell 14, 1610–1623.

Conibear E, Stevens TH (2000). Vps52p, Vps53p, and Vps54p form a novel multisubunit complex required for protein sorting at the yeast late Golgi. Mol Biol Cell 11, 305–323.

Dilcher M, Kohler B, von Mollard GF (2001). Genetic interactions with the yeast Q-SNARE VTI1 reveal novel functions for the R-SNARE YKT6. J Biol Chem 276, 34537–34544.
Dilcher M, Veith B, Chidambaram S, Hartmann E, Schmitt HD, Fischer von Mollard G (2003). Use1p is a yeast SNARE protein required for retrograde traffic to the ER. EMBO J 22, 3664–3674.
Farber SA, Pack M, Ho SY, Johnson ID, Wagner DS, Dosch R, Mullins MC, Hendrickson HS, Hendrickson EK, Halpern ME (2001). Genetic analysis of digestive physiology using fluorescent phospholipid reporters. Science 292, 1385–1388.
Fares H, Greenwald I (2001a). Genetic analysis of endocytosis in *Caenorhabditis elegans*: coelomocyte uptake defective mutants. Genetics 159, 133–145.
Fares H, Greenwald I (2001b). Regulation of endocytosis by CUP-5, the *Caenorhabditis elegans* mucolipin-1 homolog. Nat Genet 28, 64–68.
Fiala JC (2005). Reconstruct: a free editor for serial section microscopy. J Microsc 218, 52–61.
Fischer von Mollard G, Stevens TH (1999). The *Saccharomyces cerevisiae* v-SNARE Vti1p is required for multiple membrane transport pathways to the vacuole. Mol Biol Cell 10, 1719–1732.
Frickenhaus S, Beszteri B (2008). Quicktree-SD. Bioinformatics, Alfred Wegener Institute for Polar and Marine Research, Bremerhaven, Germany. Available at: http://epic.awi.de/Publications/Fri2008j.pdf.
Fridmann-Sirkis Y, Kent HM, Lewis MJ, Evans PR, Pelham HR (2006). Structural analysis of the interaction between the SNARE Tlg1 and Vps51. Traffic 7, 182–190.
Grant B, Hirsh D (1999). Receptor-mediated endocytosis in the *Caenorhabditis elegans* oocyte. Mol Biol Cell 10, 4311–4326.
Guermonprez H, Smertenko A, Crosnier MT, Durandet M, Vrielynck N, Guerche P, Hussey PJ, Satiat-Jeunemaitre B, Bonhomme S (2008). The POK/AtVPS52 protein localizes to several distinct post-Golgi compartments in sporophytic and gametophytic cells. J Exp Bot 59, 3087–3098.
Hay JC, Klumperman J, Oorschot V, Steegmaier M, Kuo CS, Scheller RH (1998). Localization, dynamics, and protein interactions reveal distinct roles for ER and Golgi SNAREs. J Cell Biol 141, 1489–1502.
Ho SY, Lorent K, Pack M, Farber SA (2006). Zebrafish fat-free is required for intestinal lipid absorption and Golgi apparatus structure. Cell Metab 3, 289–300.
Howe K, Bateman A, Durbin R (2002). QuickTree: building huge neighbor-joining trees of protein sequences. Bioinformatics 18, 1546–1547.
Hsu SC, TerBush D, Abraham M, Guo W (2004). The exocyst complex in polarized exocytosis. Int Rev Cytol 233, 243–265.
Jahn R, Scheller RH (2006). SNAREs—engines for membrane fusion. Nat Rev Mol Cell Biol 7, 631–643.
Kamath RS, Martinez-Campos M, Zipperlen P, Fraser AG, Ahringer J (2001). Effectiveness of specific RNA-mediated interference through ingested double-stranded RNA in *Caenorhabditis elegans*. Genome Biol 2, 231–237.
Katoh K, Kuma K, Toh H, Miyata T (2005). MAFFT version 5: improvement in accuracy of multiple sequence alignment. Nucleic Acids Res 33, 511–518.
Kloepper TH, Kienle CN, Fasshauer D (2008). SNAREing the basis of multicellularity: consequences of protein family expansion during evolution. Mol Biol Evol 25, 2055–2068.
Koumandou VL, Dacks JB, Coulson RM, Field MC (2007). Control systems for membrane fusion in the ancestral eukaryote; evolution of tethering complexes and SM proteins. BMC Evol Biol 7, 29.
Kubota Y, Sano M, Goda S, Suzuki N, Nishiwaki K (2006). The conserved oligomeric Golgi complex acts in organ morphogenesis via glycosylation of an ADAM protease in *C. elegans*. Development 133, 263–273.
Lang T, Jahn R (2008). Core proteins of the secretory machinery. Handb Exp Pharmacol 2008(184), 107–127.
Laufman O, Kedan A, Hong W, Lev S (2009). Direct interaction between the COG complex and the SM protein, Sly1, is required for Golgi SNARE pairing. EMBO J 28, 2006–2017.
Lee RC, Hammell CM, Ambros V (2006). Interacting endogenous and exogenous RNAi pathways in *Caenorhabditis elegans*. RNA 12, 589–597.
Liewen H, Meinhold-Heerlein I, Oliveira V, Schwarzenbacher R, Luo G, Wadle A, Jung M, Pfreundschuh M, Stenner-Liewen F (2005). Characterization of the human GARP (Golgi associated retrograde protein) complex. Exp Cell Res 306, 24–34.
Lupashin VV, Pokrovskaya ID, McNew JA, Waters MG (1997). Characterization of a novel yeast SNARE protein implicated in Golgi retrograde traffic. Mol Biol Cell 8, 2659–2676.
Maekawa M, Inoue T, Kobuna H, Nishimura T, Gengyo-Ando K, Mitani S, Arai H (2009). Functional analysis of GS28, an intra-Golgi SNARE, in *Caenorhabditis elegans*. Genes Cells 14, 1003–1013.
Mallard F, Tang BL, Galli T, Tenza D, Saint-Pol A, Yue X, Antony C, Hong W, Goud B, Johannes L (2002). Early/recycling endosomes-to-TGN transport involves two SNARE complexes and a Rab6 isoform. J Cell Biol 156, 653–664.
Mello CC, Kramer JM, Stinchcomb D, Ambros V (1991). Efficient gene transfer in *C. elegans*: extrachromosomal maintenance and integration of transforming sequences. EMBO J 10, 3959–3970.
Nicot AS, Fares H, Payrastre B, Chisholm AD, Labouesse M, Laporte J (2006). The phosphoinositide kinase PIKfyve/Fab1p regulates terminal lysosome maturation in *Caenorhabditis elegans*. Mol Biol Cell 17, 3062–3074.
O'Brien KP, Tapia-Paez I, Stahle-Backdahl M, Kedra D, Dumanski JP (2000). Characterization of five novel human genes in the 11q13-q22 region. Biochem Biophys Res Commun 273, 90–94.
Orci L, Ravazzola M, Volchuk A, Engel T, Gmachl M, Amherdt M, Perrelet A, Sollner TH, Rothman JE (2000). Anterograde flow of cargo across the Golgi stack potentially mediated via bidirectional "percolating" COPI vesicles. Proc Natl Acad Sci USA 97, 10400–10405.
Panic B, Whyte JR, Munro S (2003). The ARF-like GTPases Arl1p and Arl3p act in a pathway that interacts with vesicle-tethering factors at the Golgi apparatus. Curr Biol 13, 405–410.
Perez-Victoria FJ, Bonifacino JS (2009). Dual roles of the mammalian GARP complex in tethering and SNARE complex assembly at the trans-Golgi network. Mol Cell Biol 29, 5251–5263.
Perez-Victoria FJ, Mardones GA, Bonifacino JS (2008). Requirement of the human GARP complex for mannose 6-phosphate-receptor-dependent sorting of cathepsin D to lysosomes. Mol Biol Cell 19, 2350–2362.
Perez-Victoria FJ, Schindler C, Magadan JG, Mardones GA, Delevoye C, Romao M, Raposo G, Bonifacino JS (2010). Ang2/fat-free is a conserved subunit of the Golgi-associated retrograde protein complex. Mol Biol Cell 21, 3386–3395.
Reggiori F, Wang CW, Stromhaug PE, Shintani T, Klionsky DJ (2003). Vps51 is part of the yeast Vps fifty-three tethering complex essential for retrograde traffic from the early endosome and Cvt vesicle completion. J Biol Chem 278, 5009–5020.
Ronquist F, Huelsenbeck JP (2003). MrBayes 3: Bayesian phylogenetic inference under mixed models. Bioinformatics 19, 1572–1574.
Rostaing P, Weimer RM, Jorgensen EM, Triller A, Bessereau JL (2004). Preservation of immunoreactivity and fine structure of adult *C. elegans* tissues using high-pressure freezing. J Histochem Cytochem 52, 1–12.
Schmitt-John T *et al.* (2005). Mutation of Vps54 causes motor neuron disease and defective spermiogenesis in the wobbler mouse. Nat Genet 37, 1213–1215.
Shestakova A, Suvorova E, Pavliv O, Khaidakova G, Lupashin V (2007). Interaction of the conserved oligomeric Golgi complex with t-SNARE Syntaxin5a/Sed5 enhances intra-Golgi SNARE complex stability. J Cell Biol 179, 1179–1192.
Short B, Haas A, Barr FA (2005). Golgins and GTPases, giving identity and structure to the Golgi apparatus. Biochim Biophys Acta 1744, 383–395.
Siniossoglou S, Pelham HR (2001). An effector of Ypt6p binds the SNARE Tlg1p and mediates selective fusion of vesicles with late Golgi membranes. EMBO J 20, 5991–5998.
Siniossoglou S, Pelham HR (2002). Vps51p links the VFT complex to the SNARE Tlg1p. J Biol Chem 277, 48318–48324.
Smith RD, Lupashin VV (2008). Role of the conserved oligomeric Golgi (COG) complex in protein glycosylation. Carbohydr Res 343, 2024–2031.
Smith RD, Willett R, Kudlyk T, Pokrovskaya I, Paton AW, Paton JC, Lupashin VV (2009). The COG complex, Rab6 and COPI define a novel Golgi retrograde trafficking pathway that is exploited by SubAB toxin. Traffic 10, 1502–1517.
Spelbrink RG, Nothwehr SF (1999). The yeast GRD20 gene is required for protein sorting in the trans-Golgi network/endosomal system and for polarization of the actin cytoskeleton. Mol Biol Cell 10, 4263–4281.
Tai G, Lu L, Wang TL, Tang BL, Goud B, Johannes L, Hong W (2004). Participation of the syntaxin 5/Ykt6/GS28/GS15 SNARE complex in transport from the early/recycling endosome to the trans-Golgi network. Mol Biol Cell 15, 4011–4022.

Treusch S, Knuth S, Slaugenhaupt SA, Goldin E, Grant BD, Fares H (2004). *Caenorhabditis elegans* functional orthologue of human protein h-mucolipin-1 is required for lysosome biogenesis. Proc Natl Acad Sci USA 101, 4483–4488.

Tsui MM, Banfield DK (2000). Yeast Golgi SNARE interactions are promiscuous. J Cell Sci 113 (pt 1), 145–152.

Tsui MM, Tai WC, Banfield DK (2001). Selective formation of Sed5p-containing SNARE complexes is mediated by combinatorial binding interactions. Mol Biol Cell 12, 521–538.

Ungar D, Oka T, Krieger M, Hughson FM (2006). Retrograde transport on the COG railway. Trends Cell Biol 16, 113–120.

VanRheenen SM, Cao X, Lupashin VV, Barlowe C, Waters MG (1998). Sec35p, a novel peripheral membrane protein, is required for ER to Golgi vesicle docking. J Cell Biol 141, 1107–1119.

VanRheenen SM, Cao X, Sapperstein SK, Chiang EC, Lupashin VV, Barlowe C, Waters MG (1999). Sec34p, a protein required for vesicle tethering to the yeast Golgi apparatus, is in a complex with Sec35p. J Cell Biol 147, 729–742.

Vanrheenen SM, Reilly BA, Chamberlain SJ, Waters MG (2001). Dsl1p, an essential protein required for membrane traffic at the endoplasmic reticulum/Golgi interface in yeast. Traffic 2, 212–231.

Volchuk A *et al*. (2004). Countercurrent distribution of two distinct SNARE complexes mediating transport within the Golgi stack. Mol Biol Cell 15, 1506–1518.

Whyte JR, Munro S (2001). The Sec34/35 Golgi transport complex is related to the exocyst, defining a family of complexes involved in multiple steps of membrane traffic. Dev Cell 1, 527–537.

Whyte JR, Munro S (2002). Vesicle tethering complexes in membrane traffic. J Cell Sci 115, 2627–2637.